Nanoscale

Accepted Manuscript

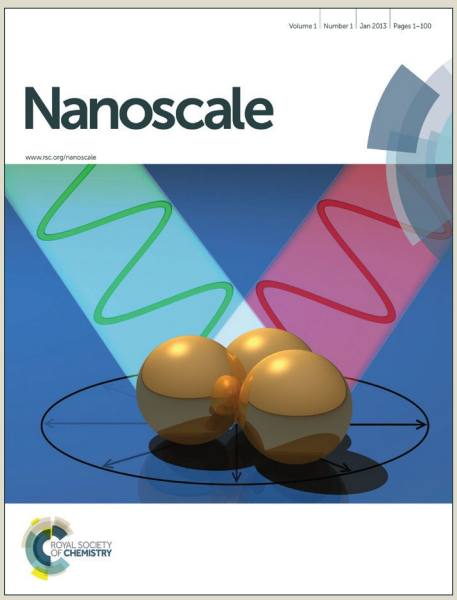

ROYAL SOCIETY OF CHEMISTRY

www.rsc.org/nanoscale

Journal Name

RSCPublishing

ARTICLE

Novel Silica Surface Charge Density Mediated Control of the Optical Properties of Embedded Optically Active Materials and Its Application for Fiber Optic pH Sensing at Elevated Temperatures

Cite this: DOI: 10.1039/x0xx00000x

Received 00th January 2012,
Accepted 00th January 2012

DOI: 10.1039/x0xx00000x

www.rsc.org/

Congjun Wang,*[ab] Paul R. Ohodnicki, Jr.,[ac] Xin Su,[a] Murphy Keller,[a] Thomas D. Brown,[a] and John P. Baltrus[a]

Silica and silica incorporated nanocomposite materials have been extensively studied for a wide range of applications. Here we demonstrate a remarkable optical effect of silica that, depending on the solution pH, amplifies or screens the optical absorption of a variety of embedded optically active materials with very distinct properties, such as plasmonic Au nanoparticles, non-plasmonic Pt nanoparticles, as well as the organic dye rhodamine B (*not* a pH indicator), coated on an optical fiber. Interestingly, the observed optical response to varying pH appears to follow the surface charge density of the silica matrix for all three different optically active materials. To the best of our knowledge, this optical effect has not been previously reported and it appears univeral in that it is likely that any optcially active material can be incorporated into the silica matrix to respond to solution pH or surface charge density variations. A direct application of this effect is for optical pH sensing which has very attractive features that can enable minimally invasive, remote, real time and continuous distributed pH monitoring. Particularly, as demonstrated here, using highly stable metal nanoparticles embedded in an inorganic silica matrix can significantly improve the capability of pH sensing in extremely harsh environments which is of increasing importance for applications in unconventional oil and gas resource recovery, carbon sequestration, and water quality monitoring etc. Our approach opens a pathway towards possible future development of robust optical pH sensors for the most demanding environmental conditions. The newly discoverd optical effect of silica also offers the potential for control of the optical properties of optically active materials for a range of other potential applications such as electrochromic devices.

Introduction

As the most abudant compound on earth and one of the most useful and versatile materials, silica (SiO_2) has been intensively investigated for a wide variety of applications ranging from construction, energy, chemical engeering, electronics, optics, telecommunications, biomedical and pharmaceutical industry, and so on. A variety of silica nano- and meso-structures has attracted significant attention to understand the properties of colloids[1] and improve the performance of important catalysts,[2] and so on.[3] Because of silica's compatibility with biological envrironments and its extremely controllabe surface chemistry, silica has been attractive for various application in biochemistry and medicine.[4, 5] These materials have also been widely used as templates for the preparation of different types of functional nanostrutures.[6, 7] Moreover, silica based hybrid materials have demonstrated attractive electronic, optical and chemical properties.[8] For example, silica has been extensively studied to enhance the properties of a myriad of nanomaterials such as tuning the optical properties of plasmonic nanoparticles,[9] providing biocompatibility and surface functionality to fluorescent semiconductor quantum dots,[10] etc. Finally, the properties of colloidal silica nanoparticles have been carefully investigated to understand their behavior under different conditions, including the surface charge density and the aggregation of these particles as a response to pH changes.[11, 12] Silica has also been utilized as a substrate material for pH sensing.[13-19]

On the other hand, as one of the most basic parameters that characterize chemical properties of aqueous solutions, the measurements of pH are important for a wide range of disciplines such as life and pharmaceutical sciences, environmental, earth and marine sciences, civil and chemical engineering, just to name a few.[20-23] While techniques for sensing pH in biological and physiological systems have noticeably matured,[22] there remains a need for new pH sensors

that can enable minimally invasive pH measurement with high temporal and spatial resolution.[24, 25] Furthermore, pH sensing in certain industrial, environmental and geological contexts remains challenging due to complicated compositions and other variables including temperature and pressure. [26-29]

Optical pH sensors demonstrate several very desirable advantages. They can be miniaturized to sub-μm dimensions, eliminate the need for mechanically rigid electrodes as well as electronic components and wiring, are not susceptible to electrical interference and do not require a separate reference sensor. They can enable continuous pH monitoring and can have potentially reduced production cost. Combined with fiber optics technology, optical pH sensors can be used for minimally invasive, remote sensing in distributed networks, and can allow broadband or multi-wavelength interrogation with the possibility of simultaneous measurements of multiple parameters with the same telemetry. However, the vast majority of the optical pH sensing materials studied to date depend on organic dyes, fluorescent molecules, and/or polymers which suffer from photobleaching and/or very limited stability at elevated temperatures.[23, 30] There has been growing interest in the development of other materials for optical pH sensing, such as silica based nanostructures functionalized with fluorescent dyes,[13-19] carbon dots,[31-34] and graphene oxide,[35] and photonic crystals.[36] But none of these systems are capable of robust operation at extreme temperatures. Optically active inorganic nanorods,[37, 38] semiconductor quantum dots[39-45] and plasmonic metal nanocrystals/nanorods[46-50] have recently emerged as potential pH sensors. Yet these nanostructures are not inherently sensitive to pH changes and they still require the presence of pH responsive but delicate molecules, polymers and/or hydrogels to induce the optical changes at difference pH values, preventing them from pH sensing applications under extreme conditions.

Here we present the investigation of the optical properties of three very different optically active materials embedded in a silica matrix as the solution pH is varied and the subsequent development of optical fiber-based nanocomposite pH sensors utilizing this newly discovered optical effect of silica that seems to be potentially applicable to any type of optically active materials. Fabricating optical fiber pH sensors with materials compatible with extreme temperature and pressure environments demonstrates robust response and excellent stability. Unlike previous reports on silica based optical pH sensors, where silica only serves as a passive substrate for other sensing materials,[13-19] the observed response in our system appears to be dominated by the properties of the silica matrix. Specifically, our observations suggest that the optical effect may be controlled by the surface charge density of silica, which can also potentially be exploited for other applications such as novel optoelectronic and electrochromic devices.

Experimental section

Preparation of silica based nanocomposite coated optical fibers.

All chemicals were purchased from Aldrich and used as received unless otherwise noted. The fabrication of the nanocomposite coated optical fibers started with the preparation of a coating solution using a sol-gel technique. Briefly, 0.04 g of $HAuCl_4$ (Alfa Aesar, 99.999 %) was mixed with 1.0 ml deionized water, 4.5 ml ethanol and 4.5 ml tetraethoxysilane (TEOS) (Alfa Aesar, 98 %). Alternatively, octyltrichlorosilane (OTCS) (97 %) was used to replace TEOS for control experiments. The mixture was stirred at 60 °C for 1 hour and kept in a N_2 glove box. To prepare an optical fiber coated with plasmonic Au nanoparticles, an optical fiber (ThorLabs, FG105LCA, Multimode Fiber, 0.22 NA, Low-OH, Ø105 μm Core, 400 - 2400 nm) was first heated in air at 550 °C for 60 minutes to remove the polymer coating and then etched in a buffered oxide HF etchant solution for 50 minutes. The etched fiber was subsequently coated with the Au/TEOS coating solution using a dip-coating approach by pulling the fiber through the solution at a rate of ~1 cm/s and then calcined at either 200 °C or 600 °C for 45 – 60 minutes in air. Calcination at 600 °C is to ensure the complete conversion of silane molecules to an inorganic SiO_2 matrix for enhanced high temperature stability. To deposit Au nanoparticle film on a planar substrate, the Au/TEOS solution was spin-coated on the substrate and heated to 200 °C for 45 min in air. The preparation of optical fibers with other optically active materials such as Pd nanoparticles was performed in a similar manner using $PdCl_2$ (99 %) as the Pd source. Rhodamine B based optical fiber was also prepared by dissovling 10 mg of rhodamine B in the coating solution and to avoid thermal degradation of the organic dye, no calcination was performed and the coated fiber was allowed to dry in air for 2 days instead. As control experiments, planar films and optical fibers were also coated with pure TEOS in H_2O/ethanol using the same procedure.

Characterization of nanocomposite optical fibers.

The optical fibers were characterized by scanning electron microscopy (SEM) using an FEI Quanta Environmental SEM equipped with a field emission gun (FEG) in low-vacuum mode with an accelerating voltage of 20 kV and a spot size of 3. Optical properties of planar films were characterized over the wavelength range of 200 – 2500nm in a transmittance and reflectance geometry using a Perkin Elmer Lambda 1050 spectrophotometer equipped with an integrating sphere. X-ray photoelectron spectroscopy (XPS) measurements were carried out using a PHI 5600ci instrument. The XPS instrument employed monochromatic Al Kα X-rays and the pass energy of the analyzer was 23.5 eV. An electron gun was used for charge neutralization. Elemental concentrations were calculated using sensitivity factors provided by the instrument manufacturer. XPS peak fitting analyses were accomplished using CasaXPS data processing software. Binding energies were referenced to the Au $4f_{7/2}$ peak at 84.0 eV.

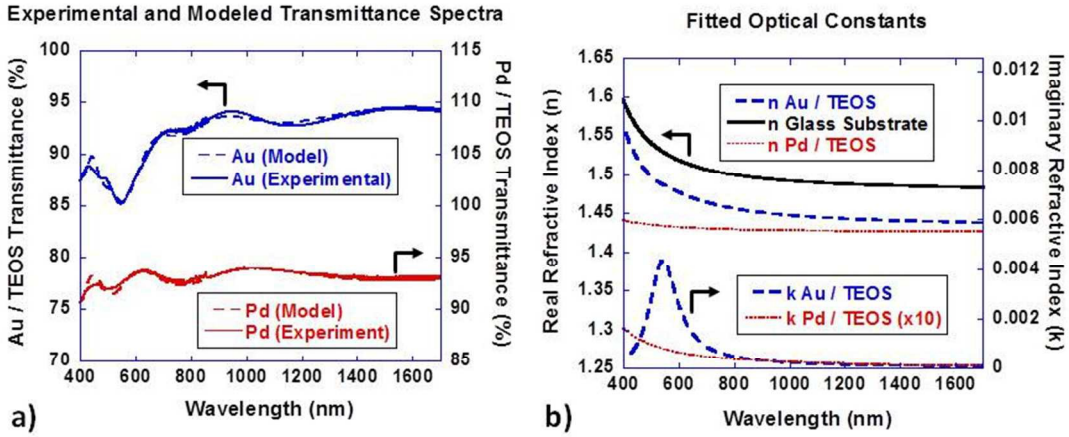

Fig 1 a) The experimentally measured and modeled transmittance spectra of a Au/TEOS and Pd/TEOS film calcined at 200 °C on a planar glass substrate. b) Corresponding fitted values of the real (*n*) and imaginary (*k*) refractive indices of the films and the glass substrate. The imaginary refractive index of the Pd film is enhanced by a factor of ten for clarity and it is essentially zero for all wavelengths for the bare glass substrate.

pH response experiments with nanocomposite optical fibers.

Most of the pH response experiments were carried out using optical fibers calcined at 200 °C, unless otherwise noted. The optical response to pH was measured by monitoring the transmission spectral changes using an OceanOptics spectrometer of an optical fiber coated with different optically active materials in a solution as the solution pH was varied by adding 0.1 M NaOH and 0.1 M H_3PO_4. The relative transmission spectra were recorded using the transmission through the optical fiber in pure H_2O at the beginning of the experiment as the background, which causes the observation that some of the relative transmission spectra shown here have > 100% transmission. Alternatively, 0.1 M KOH and 0.1 M H_2SO_4 were also used for pH adjustment. NaCl was used to test the response to changes in the refractive index of the solution and to demonstrate the capability of pH response using optically active materials incorporated silica optical fibers in high salinity conditions, which are also ubiquitous in downhole and geological environments. Finally, experiments at temperatures up to 80 °C at 1 atmospheric pressure were carried out to demonstrate the potential of these materials for high temperature pH sensing. A schematic of the pH response experimental setup is shown in Figure S1†.

Results and discussion

Optical properties of Au/TEOS films.

Measured transmittance spectra are presented in Figure 1a for Au/TEOS and Pd/TEOS films calcined at 200 °C on planar substrates. At wavelengths longer than ~800 nm, the optical spectra show clear interference fringes due to the mismatch in the real part of the refractive index (*n*) of the films as compared to the glass substrate from which both the film thickness and effective refractive indices can be estimated.[51] At shorter wavelengths, a transmittance minimum can be resolved for the Au/TEOS film which is associated with the localized surface plasmon resonance absorption (LSPR) peak of Au nanoparticles that have formed during the calcination step. In contrast, a broadband reduction in transmission that becomes more significant with decreasing wavelength is observed for the Pd/TEOS film and no evidence for a localized surface plasmon resonance is observed as expected. To extract the effective optical constants and the effective thickness of the Au/TEOS and Pd/TEOS nanocomposite films, the dielectric constant of the glass substrate was modeled as a Tauc-Lorentz absorption peak to account for the interband UV absorption while the Au/TEOS film was modeled similarly but with an additional Lorentz absorption peak in the visible range to account for the Au LSPR absorption.[52, 53] The Pd/TEOS film was modeled as a Maxwell-Garnett effective medium layer using tabulated values of the optical constant of bulk Pd metal.[54] The films were assumed to be a smooth, monolithic layer on one side of the glass substrate and a standard Levenberg-Marquardt algorithm was used to optimize the fit with the adjustable parameters associated with the amplitude and detailed shape of each absorption peak as well as the film thickness. For the Pd/TEOS film, the volume fraction of Pd particles was an additional adjustable parameters included. The empirically modeled transmittance spectra derived in this way are presented in Figure 1a along with the experimentally measured spectra showing good agreement. The fitted values of the real (*n*) and imaginary (*k*) optical constants of the Au/TEOS and Pd/TEOS films are also presented in Figure 1b along with the corresponding refractive index of the glass substrate. The smaller real refractive index of the Au/TEOS and Pd/TEOS film as compared to the glass substrate is important in dictating the interaction of the guided light with the sensing layer when integrated with an optical fiber based sensor platform as described in more detail in previous publications.[55-57] The pronounced peak in the imaginary part of the refractive index for Au/TEOS and the corresponding broadband increase with decreasing wavelengths for Pd/TEOS give rise to the LSPR absorption peak and broadband absorption, respectively, monitored during the sensor tests described in detail below.

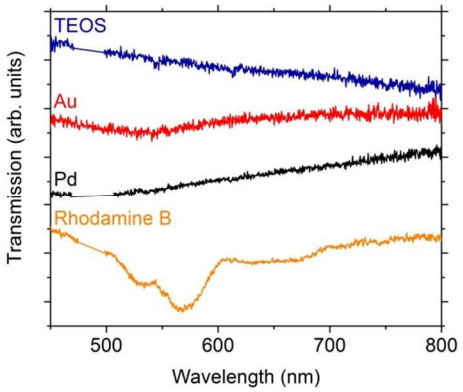

Fig 2 The relative transmission spectra of 4 optical fibers coated with pure TEOS (blue), Au nanoparticles/TEOS (red), Pd nanoparticles/TEOS (black), all calcined at 200 ℃, and rhodamine B/TEOS (orange) dried at room temperature. Note that rhodamine B is not a pH indicator dye. An artifact associated with the spectral intensity of the light source and non-uniform gain of the spectrometer in the range of 470 to 500 nm is removed for clarity for the spectra of pure TEOS, Pd/TEOS and rhodamine B/TEOS coated fibers. The spectra are offset vertically for clarity.

Optical response to pH using optically active materials embedded silica coated optical fibers.

Similar to the films deposited on planar substrates, the formation of Au nanoparticles after calcination of fabricated optical fibers based on Au/TEOS layers is confirmed by the appearance of the characteristic plasmon absorption band around 530 nm (Figure 2). The existence of Au nanoparticles is also verified by the SEM images of these fibers (Figure S2†). Similarly, a broadband absorption feature associated with the Pd nanocrystals is observed for Pd coated fibers (Figure 2) and the aborption feature for rhodamine B is clearly visible for rhodamine B coated fibers (Figure 2). In contrast, the transmission spectrum of a fiber treated with pure TEOS is essentially featureless showing a slight broadband increase as compared to the precalcination state in the visible spectral range as would be expected (Figure 2).

To demonstrate the optical response to varying pH of the plasmonic Au nanocrystal coated optical fiber, the relative transmission spectra of the fiber at various pH values are shown in Figure 3a. The plasmon absorption band grows significantly as pH increases which appears to be an overall amplification of

(a)

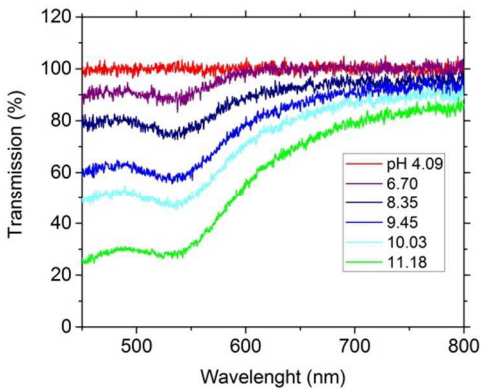

(b)

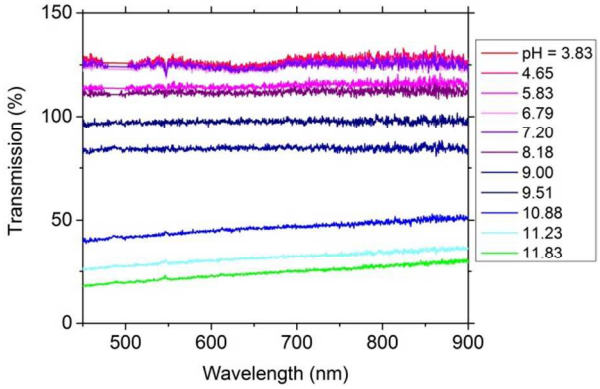

(c)

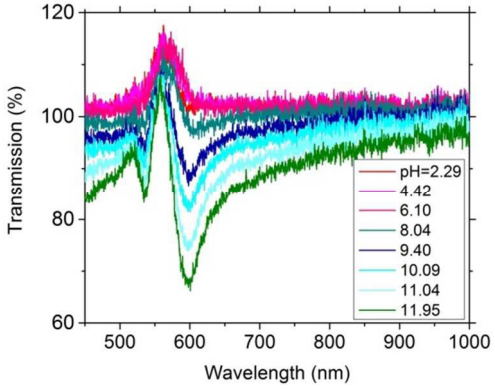

(d)

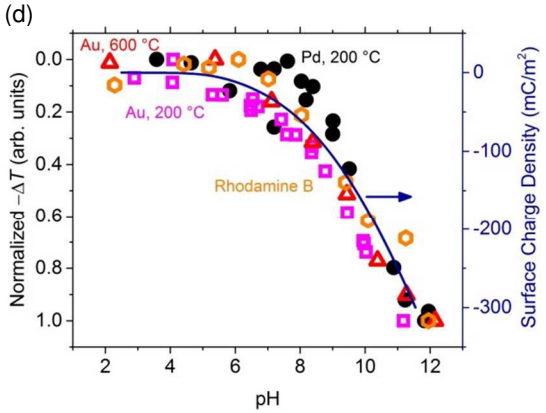

Fig. 3 The relative transmission spectra of (a) a Au nanoparticles (b) a Pd nanoparticles and (c) a rhodamine B coated optical fibers at different pH values. An artifact near 480 nm for some of the spectra in (b) is masked for clarity. (d)

Normalized change in transmission as a function of solution pH (symbols and left *y* axis) at the peak plasmon absorption band wavelengths of 525 and 530 nm for the Au coated fibers calcined at 200 ℃ (magenta open squares) and 600 ℃ (red open triangles), respectively, at 450 nm for the Pd coated fiber (black solid circles) calcined at 200 ℃, and at 600 nm for the rhodamine B/TEOS (orange open hexagons) coated fiber. The blue solid curve (right *y* axis) is the calculated surface charge density of silica as a function of pH based on the Stern model as described in the main text.

the measured extinction (Figure 3a). A similar response is also observed for Au/TEOS coated fibers calcined at 600 °C (Figure S5†). Previous reports have explained the modifications to the plasmon absorption band with varying pH values as a result of changes in the refractive index of the surrounding matrix phase resulting in absorption peak shifts,[47] as well as the change in the coupling of the optical properties of individual nanoparticles due to changes in clustering or assembly behavior.[47-50] Similarly, shifts to the plasmon absorption band have been reported as a result of charge transfer to and from the metallic nanoparticles during elevated temperature gas sensing.[51] Shifting and dampening/broadening of the absorption peak with increasing temperatures has also been discussed as a result of changes to the effective particle volume and resistivity associated with increasing temperatures.[58]

However, in the case of the Au-nanoparticle incorporated in a silica matrix coated optical fiber described here, only changes in the absorption peak intensity can be observed and no spectral shift or broadening/narrowing can be resolved suggesting an alternative mechanism for observed sensing responses. More importantly, additional evidence of an alternative mechanism is the observation that replacement of Au nanoparticles with Pd can result in qualitatively similar responses to pH that strikingly mimic those measured for Au nanoparticles (Figure 3b). Even more interestingly, an optical fiber coated with the organic dye rhodamine B again demonstrates nearly identical response (Figure 3c), with increasing molecular absorption band intensity as pH increases. We note that rhodamine B is *not* a pH indicator dye and the molecule alone is only slightly sensitive to pH when pH is < 6, where a slight red-shift is observed with decreasing pH (Figure S6).[59] The response observed here is fundamentally different from the pH sensitivity of rhodamine B because, 1) the response is much more pronounced in basic pH ranges where the dye itself is insensitive to pH and 2) the optical response is the change in the absorption band intensity rather than spectral shift (Figure S6).[59] In the relative transmission spectra of rhodamine B coated fiber, the transmission at ~560 nm seems to vary little with respect to pH leading to a strange spectral profile at high pH values. This is not fully understood and is certainly interesting for future studies to identify the origin for this observation.

The most significant observation is that when normalized to the maximum change in transmission (Figure 3d), the response from 3 very *distinct* materials, plasmonic Au nanoparticles (calcined at 200 and 600 °C), non-plasmonic metallic Pd nanoparticles (calcined at 200 °C) and the organic rhodamine B, follows the same trend as pH is varied. Because light absorption for the 3 materials is fundamentally different, the absorption of Au nanoparticles arises from plasmon resonance, whereas the Pd nanoparticles do not exhibit a plasmon resonance absorption in the visible spectral range and the absorption of rhodamine B is due to molecular electronic transition, the primary active mechanism cannot be based upon the standard theories used to describe localized surface plasmon resonance sensor responses.[60-66] Additionally, these observations prove that the optical response is not a result of the change of the refractive index of the solution (n_s) or the matrix phase (n_m). Rather, the observed response that is independent of the exact type of optically active material embedded in the silica matrix strongly suggests that it has to be dominated by silica, which will be discussed in more detail in the next section.

To ensure that the strong optical response is associated with the optically active materials embedded in the silica matrix and is a response towards changes in pH rather than a parameter that is correlated with the pH (e.g. solution refractive index, concentration of a particular ionic species, etc.), a series of control experiments was performed. Firstly, several fibers coated with pure TEOS were tested and the fibers were observed to exhibit no experimentally significant response to solution pH changes (Figure S9†). Secondly, an experiment using 0.1 M H_2SO_4 and 0.1 M KOH as the acid/base pair for pH adjustment was carried out and the Au/TEOS coated fiber demonstrated qualitatively similar response to pH irrespective of specific acid/base pairs used (Figure S10†). Finally, despite the convincing observation that Pd and rhodamine B coated fibers, whose absorption is not affected by solution refractive index, exhibit qualitatively similar optical response to that of Au coated fibers, additional control experiments were nevertheless performed to verify the irrelevance of the change in the refractive index n_s of the solution to the observed optical response (Figures S11 and S12). These control experiments offer indisputable evidence that the optical response of the optically active materials embedded silica coated fibers is truly a result of variation of solution pH.

Mechanism of the optical response.

The striking observation that all 3 distinct materials, Au, Pd, and rhodamine B, exhibits identical optical response to varying pH (Figure 3) indicates that standard mechanisms used to explain the response of LSPR based optical sensors cannot be applied to the sensors under investigation here, namely (1) refractive index of the surrounding matrix or solution phase, (2) free carrier density of the plasmonic nanoparticles, and (3) damping frequency of free carriers in the plasmonic nanoparticles.[51, 58, 64-66] As such, an alternative mechanism is proposed for which several related phenomena reported in the literature may provide some insights.[67-70] In one case, the scattering of silica-based particles has been demonstrated to depend upon a local change in effective refractive index surrounding the particles[67] which could be affected by solution phase pH due to surface charging effects and the formation of an associated depletion layer at the matrix/solution interface.[12] In another case, electrochemical experiments of Au nanoparticles illustrated a dependence of LSPR absorption peak position and magnitude on (1) charge transfer between the particles and the solution, (2) an absorbing surface layer of depleted charge carrier concentration at the particle surface, and (3) a charged depletion region in the surrounding solution phase to achieve overall charge neutrality.[70] The experimental results reported here suggest that an essential role is played by the silica-based matrix, particularly in light of the observation that replacement of plasmonic Au nanoparticles with Pd or the organic dye rhodamine B exhibits a qualitatively similar optical response trend with pH and broadband responses consistent with "amplification" of absorption by Au and Pd nanoparticles

as well as rhodamine B molecules at increasing pH values (Figure 3). Careful examination of the pH dependent optical response of different fibers calcined at different temperatures (200 and 600 °C) and with different materials (Au, Pd and rhodamine B) also reveals that the optical response shows a remarkable similarity to the calculated pH dependent surface charge density of silica based on the 1 – pK basic Stern model[11, 12] with a total site density $\Gamma_0 = 8$ nm^{-2}, a Stern capacitance C_S = 2.9 F/m^2, an ionization constant pK = 7.6 and an ionic strength $I = 5 \times 10^{-2}$ M, providing further evidence for the importance of the matrix, in particular, the surface charging of silica, in the measured response (Figure 3d). The optical response at 80 °C in saturated NaCl solution showing enhanced sensitivity in low pH ranges (Figure 4) also correlates with the calculated surface charge density under the same conditions (Figure S13†), exhibiting an enhanced sensitivity under high ionic strength and elevated temperature conditions, which can be potentially exploited to further optimize the performance of these sensor in harsh environments. A discrepancy between the optical response and the calculated surface charge density in Figure S9† could potentially be attributed to the neglect of specific binding of ions at very high ionic strengths.[11]

Surface charging properties of the silica surface can be readily controlled by surface functionalization.[71] In support of a potential mechanism associated with surface charging, OTCS was substituted for the standard TEOS as the precursor for the matrix material (Figures S14 and S15†). This was observed to completely eliminate any measurable optical response with changing pH conditions (Figure S16†) presumably because the surface is now terminated with octyl groups that can no longer be charged.[71] This observation provides more support to the notion that surface charging may indeed be playing a central role.

This exceptional optical effect is very likely applicable to any type of light aborbers embedded in a silica matrix, which would open up tremendous opportunity to manipulate the optical properties of a vast variety of materials. Novel optical effects that result from the surface charge density variation on silica can also prove to be valuable because the surface properties of silica can be readily controlled by chemical functionalization or electrochemistry, which can enable the adjustment of the optical properties and associated responses of optically-active-materials-incorporated matrices of this type for enhanced sensing and potentially even other applications such as electrochromic devices.

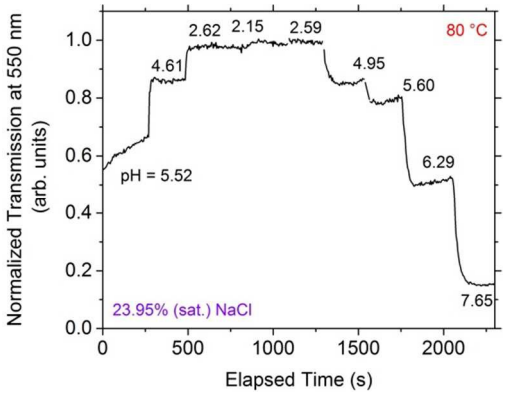

Fig. 4 Optical pH response of a plasmonic Au/TEOS coated optical fiber (calcined at 200 °C) at 80 °C and in saturated NaCl solution plotted as the transmission at the plasmon peak at 550 nm as a function of experiment time when the pH of the solution is repeatedly varied in neutral to acidic range. The pH of the solution is indicated in the figure.

Demonstration of robust pH sensing at elevated temperatures and in salt saturated solutions.

A direct application of the observed effect is optical pH sensing. Indeed, the silica based optical fiber is responsive in a wide pH range from at least 2 to 12 with higher sensitivity towards basic pH values as the optical change is more significant under high pH conditions (Figure 3d). However, these fibers have not been optimized and it is anticipated that the sensitivity at acidic pH values can be further improved through the sensor fabrication process and surface functionalization of the sensing layer. The response of the optical fiber pH sensor is rapid (response time on the order of 10s of seconds, which presumably is limited by the time needed to achieve equilibration[11, 72]), and highly reversible (the fiber sensor remains highly responsive after repeated experiments) (Figures 4, 5, S7 and S8).

Additionally, metal nanoparticle based optically active materials used in our experiments are highly stable at elevated temperatures. For example, Au nanoparticles are well-known to be chemically inert with a melting temperature approaching 1000 °C and the silica-based polymer matrix is anticipated to be stable at temperatures of at least the calcination temperature of 200 °C, and likely at much higher temperatures of 300 °C or greater. We have also fabricated Au/TEOS coated sensors calcined at 600 °C (Figure S3†), for which XPS characterization provides evidence for the decomposition of TEOS to SiO_2 (Figure S4†). Their similar pH responses (Figures 3d and S5†) further strengthens claims for the stability of these sensors at extreme temperatures.

To demonstrate the potential of these optical fibers for pH sensing in harsh environments, pH sensing experiments using the plasmonic Au in silica coated optical fiber at 80 °C and in saturated NaCl solutions is carried out. As illustrated in Figure 4, these fibers show robust responses under these conditions at neutral to acidic pH ranges. The temperature of 80 °C utilized in the current test is only limited by the fact that it is approaching the solution boiling temperature at 1 atmospheric pressure and the sensing material is expected to be stable at significantly higher temperatures than the testing conditions employed. We acknowledge that the main limitation of any silica optical fiber based sensor is the incompatibility of silica with strong base and HF solutions, which would require different materials to enable robust pH sensing under those specific conditions. To confirm the expected stability and responsiveness at elevated pressures, these fibers will be tested at elevated pressures in the near future with a reactor that is currently being built. On occasion, a drift in the optical response has been observed over time which may be related to the potential drift observed in colloidal metal oxide particles during acid/base titration experiments (Figure S11†),[11, 72] because of the correlation between the sensing response and the surface charging of the silica matrix. Further optimization of the fiber fabrication and sensing material deposition parameters may help minimize or eliminate the drift. Additionally, like many types of sensors, the response of our optical fiber based pH sensors can be influenced by a variety of experimental and environmental conditions. As just one example, the pH itself is dependent on temperature which would require additional calibration and development of the optical pH sensors based on the silica nanocomposite coated fibers. A temperature dependence of sensor transmission has indeed been observed at

fixed pH values that is not in complete agreement with expectations based solely upon temperature dependent optical constants of Au and silica as reported in our prior work.[58] This observation is currently the subject of additional investigations and will be discussed in future publications.

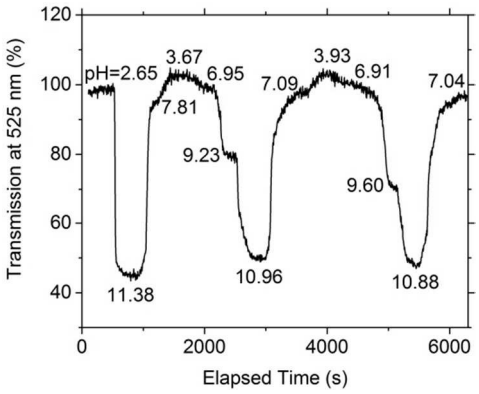

Fig. 5 The relative transmission at the plasmon absorption peak 525 nm of a Au nanoparticle/TEOS coated optical fiber calcined at 200 ℃ as a function of time as pH is varied, showing rapid, robust and reversible responses to pH change in a wide range at room temperature. The solution pH is indicated in the figure.

Conclusions

We have successfully demonstrated a novel silica surface charge density mediated control of the optical properties of 3 very distinct optically active materials: plasmonic Au nanoparticle, Pd nanoparticle and rhodamine B. The optical response of the optically active materials incorporated silica coated optical fiber to varying pH is rapid, robust, reversible, and sensitive towards a wide pH range. Our investigations also provide confidence that the optical response is associated with the effective optical extinction of the diverse optically active materials responding to the change in solution pH rather than other possible parameters such as the change in the refractive index *n* of the solution or the specific acid/base pairs. The pH response mechanism is proposed to be associated with an interaction between the solution and the silica matrix. In particular, it is proposed that the change in the surface charge density of the silica-based matrix surrounding the optically active materials in response to solution-phase pH leads to the observed optical effects which have not been reported previously. This effect is likely to be universal and could potentially enable the control of the optical properties of different types of light absobers embedded in a silica matrix. A direct application of this newly discovered phenomenon is optical pH sensing. For Au and Pd based optical fibers, because of the elimination of the delicate organic materials, these fibers demonstrate excellent potential for pH sensing at elevated temperature and in saturated salt solutions. These properties are essential for applications in high temperature and high pressure conditions and may overcome the limitations of previously existing classes of pH sensing materials. Additional in-depth investigation is currently underway to better understand the detailed mechanistic origin and to further improve the optical response with tailored performance to specific applications via careful control of the surface chemistry by selective functionalization of the surfaces. Experiments at much higher temperatures and pressures have also been initiated to demonstrate pH sensing under extreme conditions. Finally, electrochromic devices using optically active materials embedded in oxide or other dielectric matrices such as the ones investigated here may also be promising for other novel electrochromic applications[73, 74] such as smart windows or displays that allow control of the optical properties of the materials by applying an electrochemical potential.

Acknowledgements

This work was supported by the U.S. Department of Energy, Office of Fossil Energy, under the Office of Oil and Natural Gas (Energy Policy Act of 2005, Section 999 Complementary Program Research) and the Strategic Center for Coal (Cross-cutting Research Program). This report was prepared as an account of work sponsored by an agency of the United States Government. Neither the United States Government nor any agency thereof, nor any of their employees, makes any warranty, express or implied, or assumes any legal liability of responsibility for the accuracy, completeness, or usefulness of any information, apparatus, product, or process disclosed, or represents that its use would not infringe privately owned rights. Reference herein to any specific commercial product, process, or service by trade name, trademark, manufacturer, or otherwise does not necessarily constitute or imply its endorsement, recommendation, or favoring by the United States Government or any agency thereof. The views and opinions of authors expressed herein do not necessarily state or reflect those of the United States Government or any agency thereof.

Notes and references

* Fax: +1-412-386-4542; Tel: +1-412-386-5815; E-mail: congjun.wang@netl.doe.gov
[a] National Energy Technology Laboratory, U.S. Department of Energy, 626 Cochrans Mill Road, Pittsburgh, PA 15236, United States.
[b] URS Corporation, P.O. Box 618, South Park, PA 15129, United States.
[c] Carnegie Mellon University, Department of Materials Science and Engineering, 5000 Forbes Avenue, Pittsburgh, PA 15213, United States.

† Electronic Supplementary Information (ESI) available: schematic of the experimental setup, SEM images of the optical fiber sensors, XPS spectra of the sensor materials, as well as additional sensing results from control experiments. See DOI: 10.1039/b000000x/

1. A. van Blaaderen, R. Ruel and P. Wiltzius, *Nature*, 1997, **385**, 321-324.
2. A. Corma, *Chemical Reviews*, 1997, **97**, 2373-2419.
3. Y. Chen, H. R. Chen and J. L. Shi, *Accounts of Chemical Research*, 2014, **47**, 125-137.
4. Y. Piao, A. Burns, J. Kim, U. Wiesner and T. Hyeon, *Advanced Functional Materials*, 2008, **18**, 3745-3758.
5. Y. W. Yang, Y. L. Sun and N. Song, *Accounts of Chemical Research*, 2014, **47**, 1950-1960.
6. F. Caruso, R. A. Caruso and H. Mohwald, *Science*, 1998, **282**, 1111-1114.
7. M. R. Jones, K. D. Osberg, R. J. Macfarlane, M. R. Langille and C. A. Mirkin, *Chemical Reviews*, 2011, **111**, 3736-3827.
8. N. J. Halas, *ACS Nano*, 2008, **2**, 179-183.

9. N. J. Halas, S. Lal, W.-S. Chang, S. Link and P. Nordlander, *Chemical Reviews*, 2011, **111**, 3913-3961.
10. O. Chen, L. Riedemann, F. Etoc, H. Herrmann, M. Coppey, M. Barch, C. T. Farrar, J. Zhao, O. T. Bruns, H. Wei, P. Guo, J. Cui, R. Jensen, Y. Chen, D. K. Harris, J. M. Cordero, Z. Wang, A. Jasanoff, D. Fukumura, R. Reimer, M. Dahan, R. K. Jain and M. G. Bawendi, *Nat Commun*, 2014, **5**.
11. M. Kobayashi, F. Juillerat, P. Galletto, P. Bowen and M. Borkovec, *Langmuir*, 2005, **21**, 5761-5769.
12. S. H. Behrens and D. G. Grier, *Journal of Chemical Physics*, 2001, **115**, 6716-6721.
13. H. Xu, J. W. Aylott, R. Kopelman, T. J. Miller and M. A. Philbert, *Anal. Chem.*, 2001, **73**, 4124.
14. A. Ray, Y. K. Lee, T. Epstein, G. Kim and R. Kopelman, *Analyst*, 2011, **136**, 3616.
15. B. Korzeniowska, R. Woolley, J. DeCourcey, D. Wencel, C. E. Loscher and C. McDonagh, *Journal of Biomedical Nanotechnology*, 2014, **10**, 1336-1345.
16. S. Wu, Z. Li, J. Han and S. Han, *Chem. Commun.*, 2011, **47**, 11276.
17. Y. Chen, H. Chen, Y. Hung, F. Chien, P. Chen and C. Mou, *RSC Adv.*, 2012, **2**, 968.
18. Y. Zhang, S. W. Y. Gong, L. Jin, S. M. Li, Z. P. Chen, M. Ma and N. Gu, *Chin. Chem. Lett.*, 2009, **20**, 969.
19. A. Lapresta-Fernandez, T. Doussineau, S. Dutz, F. Steiniger, A. J. Moro and G. J. Mohr, *Nanotechnology*, 2011, **22**, 415501.
20. J. Lin, *Trends Anal. Chem.*, 2000, **19**, 541.
21. O. S. Wolfbeis, *Anal. Chem.*, 2002, **74**, 2663.
22. O. Korostynska, K. Arshak, E. Gill and A. Arshak, *IEEE Sens. J.*, 2008, **8**, 20.
23. D. Wencel, T. Abel and C. McDonagh, *Analytical Chemistry*, 2014, **86**, 15-29.
24. M. I. J. Stich, L. H. Fischer and O. S. Wolfbeis, *Chem. Soc. Rev.*, 2010, **39**, 3102.
25. M. Schäferling, *Angew. Chem., Int. Ed.*, 2012, **51**, 3532.
26. R. G. Bates, *Journal of Research of the National Bureau of Standards Section a-Physics and Chemistry*, 1962, **66**, 179-+.
27. L. W. Niedrach, *Science*, 1980, **207**, 1200-1202.
28. A. E. Hopkins, K. S. Sell, A. L. Soli and R. H. Byrne, *Marine Chemistry*, 2000, **71**, 103-109.
29. D. Bortoluzzi, C. Cinquemani, E. Torresani and S. Spilimbergo, *Journal of Supercritical Fluids*, 2011, **56**, 6-13.
30. T. Berbasova, M. Nosrati, C. Vasileiou, W. J. Wang, K. Sing, S. Lee, I. Yapici, J. H. Geiger and B. Borhan, *Journal of the American Chemical Society*, 2013, **135**, 16111-16119.
31. S. Qu, H. Chen, X. Zheng, J. Cao and X. Liu, *Nanoscale*, 2013, **5**, 5514.
32. Y. J. Heo and S. Takeuchi, *Adv. Healthcare Mater.*, 2013, **2**, 43.
33. W. Shi, X. Li and H. Ma, *Angew. Chem., Int. Ed.*, 2012, **51**, 6432.
34. F. Du, Y. Ming, F. Zeng, C. Yu and S. Wu, *Nanotechnology*, 2013, **24**, 365101.
35. L. A. Yan, Y. N. Chang, W. Y. Yin, X. D. Liu, D. B. Xiao, G. M. Xing, L. N. Zhao, Z. J. Gu and Y. L. Zhao, *Physical Chemistry Chemical Physics*, 2014, **16**, 1576-1582.
36. J. Shin, P. V. Braun and W. Lee, *Sens. Actuators, B*, 2010, **150**, 183.
37. L. Sun, H. Peng, M. I. J. Stich, D. Achatz and O. S. Wolfbeis, *Chem. Commun.*, 2009, 5000.
38. L. Xie, Y. Qin and H. Chen, *Anal. Chem.*, 2012, **84**, 1969.
39. P. T. Snee, R. C. Somers, G. Nair, J. P. Zimmer, M. G. Bawendi and D. G. Nocera, *Journal of the American Chemical Society*, 2006, **128**, 13320-13321.
40. M. Tomasulo, I. Yildiz and F. M. Raymo, *Journal of Physical Chemistry B*, 2006, **110**, 3853-3855.
41. I. L. Medintz, M. H. Stewart, S. A. Trammell, K. Susumu, J. B. Delehanty, B. C. Mei, J. S. Melinger, J. B. Blanco-Canosa, P. E. Dawson and H. Mattoussi, *Nature Materials*, 2010, **9**, 676-684.
42. J. D. Krooswyk, C. M. Tyrakowski and P. T. Snee, *Journal of Physical Chemistry C*, 2010, **114**, 21348-21352.
43. X. J. Wang, C. Boschetti, M. J. Ruedas-Rama, A. Tunnacliffe and E. A. H. Hall, *Analyst*, 2010, **135**, 1585-1591.
44. R. C. Somers, R. M. Lanning, P. T. Snee, A. B. Greytak, R. K. Jain, M. G. Bawendi and D. G. Nocera, *Chemical Science*, 2012, **3**, 2980-2985.
45. E. Kharlampieva, V. Kozlovskaya, O. Zavgorodnya, G. D. Lilly, N. A. Kotov and V. V. Tsukruk, *Soft Matter*, 2010, **6**, 800-807.
46. Z. Bai, R. Chen, P. Si, Y. Huang, H. Sun and D. Kim, *ACS Appl. Mater. Interface*, 2013, **5**, 5856.
47. V. Kozlovskaya, E. Kharlampieva, B. P. Khanal, P. Manna, E. R. Zubarev and V. V. Tsukruk, *Chemistry of Materials*, 2008, **20**, 7474-7485.
48. Z. H. Sun, W. H. Ni, Z. Yang, X. S. Kou, L. Li and J. F. Wang, *Small*, 2008, **4**, 1287-1292.
49. H. Xia, G. Su and D. Wang, *Angewandte Chemie International Edition*, 2013, **52**, 3726-3730.
50. I. Tokarev, I. Tokareva and S. Minko, *Acs Applied Materials & Interfaces*, 2011, **3**, 143-146.
51. P. R. Ohodnicki, C. J. Wang, S. Natesakhawat, J. P. Baltrus and T. D. Brown, *Journal of Applied Physics*, 2012, **111**, 064320.
52. M. P. Buric, P. Ohodnicki and B. Chorpening, *Proceedings SPIE 8816, Nanoengineering: Fabrication, Properties, Optics, and Devices X*, 2013, 88160N.
53. M. Buric, P. R. Ohodnicki and B. Chorpening, *Proceedings SPIE 9202, Photonics Applications for Aviation, Aerospace, Commercial, and Harsh Environments V*, 2014, 92021I-92021I-92029.
54. E. Palik, *Handbook of Optical Constants of Solids*, Elsevier, 1998.
55. M. P. Buric, P. R. Ohodnicki and J. Duy, *Proceedings SPIE 8463, Nanoengineering: Fabrication, Properties, Optics, and Devices IX*, 2012, 84630D-84630D-84614.
56. Z. L. Poole, P. Ohodnicki, R. Chen, Y. Lin and K. P. Chen, *Opt. Express*, 2014, **22**, 2665-2674.
57. Z. L. Poole, P. Ohodnicki, M. Buric, A. Yan, S. Riyadh, Y. Lin and K. P. Chen, *Proceedings SPIE 9161, Nanophotonic Materials XI*, 2014, 91610P-91610P-91610.
58. P. R. Ohodnicki, M. P. Buric, T. D. Brown, C. Matranga, C. J. Wang, J. Baltrus and M. Andio, *Nanoscale*, 2013, **5**, 9030-9039.
59. I. L. Arbeloa and P. R. Ojeda, *Chemical Physics Letters*, 1981, **79**, 347-350.
60. M. A. El-Sayed, *Accounts of Chemical Research*, 2001, **34**, 257-264.
61. K. L. Kelly, E. Coronado, L. L. Zhao and G. C. Schatz, *Journal of Physical Chemistry B*, 2003, **107**, 668-677.

62. H. Chen, L. Shao, Q. Li and J. Wang, *Chemical Society Reviews*, 2013, **42**, 2679-2724.
63. D. Buso, M. Post, C. Cantalini, P. Mulvaney and A. Martucci, *Advanced Functional Materials*, 2008, **18**, 3843-3849.
64. N. A. Joy, C. M. Settens, R. J. Matyi and M. A. Carpenter, *Journal of Physical Chemistry C*, 2011, **115**, 6283-6289.
65. A. Tittl, H. Giessen and N. Liu, *Nanophotonics*, 2014, **3**, 157-180.
66. L. Shao, Q. F. Ruan, R. B. Jiang and J. F. Wang, *Small*, 2014, **10**, 802-811.
67. L. M. Liz-Marzan, M. Giersig and P. Mulvaney, *Langmuir*, 1996, **12**, 4329-4335.
68. T. Ung, M. Giersig, D. Dunstan and P. Mulvaney, *Langmuir*, 1997, **13**, 1773-1782.
69. C. Novo, A. M. Funston, A. K. Gooding and P. Mulvaney, *Journal of the American Chemical Society*, 2009, **131**, 14664-+.
70. T. Sannomiya, H. Dermutz, C. Hafner, J. Voros and A. B. Dahlin, *Langmuir*, 2010, **26**, 7619-7626.
71. R. P. Bagwe, L. R. Hilliard and W. H. Tan, *Langmuir*, 2006, **22**, 4357-4362.
72. M. Schudel, S. H. Behrens, H. Holthoff, R. Kretzschmar and M. Borkovec, *Journal of Colloid and Interface Science*, 1997, **196**, 241-253.
73. C. Wang, M. Shim and P. Guyot-Sionnest, *Science*, 2001, **291**, 2390-2392.
74. A. Llordes, G. Garcia, J. Gazquez and D. J. Milliron, *Nature*, 2013, **500**, 323-326.